Cobalt Toxicity Induces Retinopathy and Optic Neuropathy in Mice

Basel Obied[1], Stephen Richard[1], Alon Zahavi[2,3], Hila Kreizman-Shefer[4], Jacob Bajar[4], Dror Fixler[5], Matea Krmpotić[5,6], Olga Girshevitz[5], and Nitza Goldenberg-Cohen[1,7]

[1]The Krieger Eye Research Laboratory, Bruce and Ruth Faculty of Medicine, Technion – Israel Institute of Technology, Haifa, Israel
[2]Department of Ophthalmology, Rabin Medical Center—Beilinson Hospital, and Laboratory of Eye Research, Felsenstein Medical Research Center, Petach Tikva, Israel
[3]Faculty of Medicine, Tel Aviv University, Tel Aviv, Israel
[4]Department of Pathology, Bnai Zion Medical Center, Haifa, Israel
[5]Faculty of Engineering and Institute of Nanotechnology and Advanced Materials, Bar Ilan University, Ramat Gan, Israel
[6]Division of Experimental Physics, Ruđer Bošković Institute, Zagreb, Croatia
[7]Department of Ophthalmology, Bnai Zion Medical Center, Haifa, Israel

Correspondence: Nitza Goldenberg-Cohen, Ophthalmology Department, Bnai Zion Medical Center, Technion, 47 Golomb St., Haifa 3339419, Israel; ncohen1@gmail.com.

Received: September 1, 2024
Accepted: November 2, 2024
Published: November 27, 2024

Citation: Obied B, Richard S, Zahavi A, et al. Cobalt toxicity induces retinopathy and optic neuropathy in mice. *Invest Ophthalmol Vis Sci.* 2024;65(13):59. https://doi.org/10.1167/iovs.65.13.59

Purpose. To explore the effect of cobalt toxicity on vision.

Methods. A total of 103 wild-type (WT) mice were injected with cobalt chloride by two routes in different concentrations: single intravenous (IV) high or low doses (total, $n = 43$); or daily repeated intraperitoneal (IP) high (three days) or low (28 days, 56 days) dose, and low-dose cobalt with added minocycline (56 days) (total, $n = 60$); 10 WT mice served as a control group. An additional group of 17 immunodeficient NOD scid gamma (NSG) mice were injected IV or IP with cobalt, and 10 NSG mice served as control. Cobalt levels were measured in blood, urine, and tears by particle-induced X-ray emission (PIXE). Macroscopic, immunohistochemical, electroretinography (ERG), and molecular studies were done.

Results. PIXE revealed cobalt elimination from the blood by two hours, with increased levels in urine but under the detection limit in tears. In the retina, ERG recordings showed decreased b-wave amplitude. Apoptosis mainly involved the inner retina, with inner retinal inflammatory reaction in both WT and less in the NSG mice. In the optic nerves, an increased microglial and astrocytic activation was noted.

Conclusions. This study demonstrated functional visual impairment with extensive inflammatory reaction secondary to cobalt toxicity in mice.

Keywords: cobalt toxicity, optic neuritis, inflammation, PIXE

Cobalt is a trace element, part of the structure of vitamin B12-cobalamin, which is essential for energy production. Cobalt toxicity is defined as blood levels above 6 µm/L.[1] It may involve multiple organs, leading to heart failure, peripheral neuropathy, and visual impairment.[2] Toxicity primarily occurs from occupational exposure[3] and consumption of beer containing cobalt sulfate as a stabilizer[4] and almost never from daily dietary intake. Cobalt intoxication has also been reported after total hip arthroplasty because of failed ceramic femoral head prosthesis with the release of cobalt metal ions into the circulation.[5] The diagnosis of cobalt toxicity is often delayed because of a low clinical index of suspicion and difficulty measuring systemic cobalt levels. Reported diagnosis of cobalt toxicity in patients with ischemic heart failure after hip arthroplasty implantation was made only after multiple cases had been reported.[6]

A few reports have described cobalt-induced visual disturbances.[1,5–14] Both the retina and optic nerve were affected. The optic nerve dysfunction was identified by hyperintensities of the optic nerves on magnetic resonance imaging. Functional studies revealed a delay in visual evoked potentials with abnormalities on electroretinography (ERG).[5] However, the pathophysiology of cobalt-related visual disturbances is only partially understood. The aim of the present study was to investigate the effect of cobalt on the visual pathway in mice, functionally and histologically, using multimodal techniques.

Methods

Study Animals

Cobalt chloride ($CoCl_2$; Sigma Aldrich, St. Louis, MO, USA) was administered to 103 wild-type mice (WT, C57Bl6) divided into two groups by route of administration and dose (Figs. 1A, 1B): single intravenous (IV) injection of a high

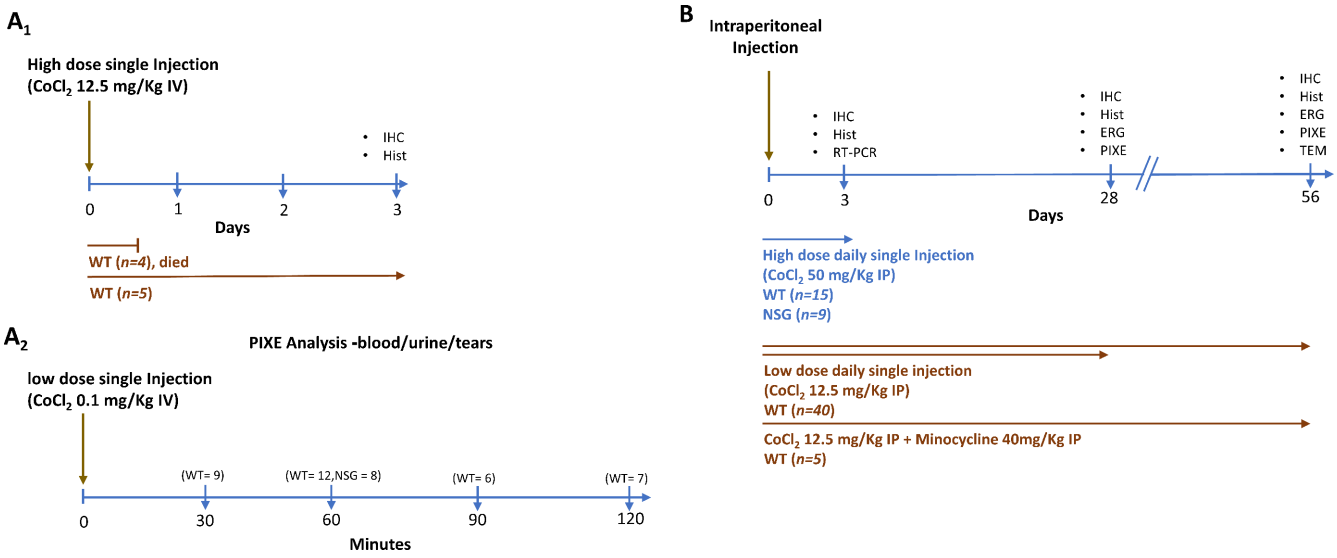

Figure 1. Experimental design. Two groups of injection: **(A)** single IV injection and **(B)** daily IP injections. The IP injected mice were further divided into four groups: (*1*) high-dose daily single injection, euthanized after three days (WT, $n = 15$; NSG, $n = 9$); (*2*) low-dose daily single injection, euthanized after 28 and 56 days (WT, $n = 40$); (*3*) low-dose single injection of CoCl2 and minocycline, euthanized after 56 days (WT, $n = 5$), (4) Non-injected control group (WT, $n = 10$; NSG, $n = 10$). Hist, histology; IHC, immunohistochemistry; EM, electron microscopy.

($n = 9$) or low ($n = 34$) dose; and repeated daily intraperitoneal (IP) injections of a high dose for three days ($n = 15$), low dose for 28, and 56 days ($n = 40$), and low dose with added minocycline for 56 days ($n = 5$). Ten WT mice served as an IP saline-injected control group. In addition, 17 immunodeficient NOD scid gamma (NSG) mice were divided into two groups: IP high daily dose injection of $CoCl_2$ for three days ($n = 9$), and a single low IV dose ($n = 8$). Another 10 NSG mice served as control.

Injection Dosages

For IV and IP administration, $CoCl_2$ was dissolved in 100 µL saline solution, and the injection dosage was calculated per kilogram mouse body weight.[15] In a 30-gr mouse, the high dose was 15 mg/mL (50 mg/kg), and low dose was 3.75 mg/mL (12.5 mg/kg), in 0.1 ml, respectively. Minocycline (M9511; Sigma-Aldrich) injection (45 mg/kg) was dissolved in 50 µL saline solution and IP injected.[16]

Injection Procedures

For IV injection, mice were placed under general anesthesia by intramuscular injection of combined ketamine/xylazine (Sigma, St. Louis, MO, USA) (80 mg/kg and 8 mg/kg, respectively). A 0.1 mL $CoCl_2$ solution was injected into the bulbar sinus. Mice were euthanized at 0, 30, 60, 90, and 120 minutes.

For IP injection, 0.1 mL $CoCl_2$ solution was injected daily. Mice were euthanized at three, 28, and 56 days.

Tear Sampling

Tears were sampled from the left eye of each subject, by placing a Schirmer Tear Test strip (IMS Euro Ltd., Stockton, UK) in the lower conjunctival fornix.

Histology

Eyes were enucleated, fixed in 4% formaldehyde, placed overnight in 30% sucrose dissolved in PBS (1X; Biological Industries, Beit HaEmek, Israel) at 4°C, and embedded in optimum cutting temperature compound (Scigen Scientific, Gardena, CA, USA). Cryosections of the globes and optic nerves (10 µm) were stained with hematoxylin and eosin (H&E) for light microscopy (Fluoview X; Olympus, Tokyo, Japan) with three consecutive sections on each slide. Retinal ganglion cells (RGCs) were counted in a magnification field ×20, three consecutive sections of every seven to 10 slides of each eye, and the mean number was calculated.

Immunohistochemistry

Retinal sections were placed on slides and washed with PBS prior to blocking with 5% fetal calf serum and 1% Triton X-100 for one hour. The sections were then incubated with the primary anti-CD45 antibody (1:200; Abcam, Cambridge, UK), anti- ionized calcium-binding adapter molecule 1(Iba-1) (1:500; Abcam), anti-NeuN (1:500; Merck Millipore, Burlington, MA, USA), and anti-glial fibrillary acidic protein (GFAP) (1:500; Abcam), at 4°C overnight. The slides were incubated with the secondary antibodies, goat anti-rabbit Alexa fluor 647 (diluted 1:1000; Abcam) and goat anti-chicken IgG NL-577 (diluted 1:200; R&D Systems-Biotest, Minneapolis, MN, USA), at room temperature for one hour. The retinal sections were counterstained with 4′, 6-diamidino-2-phenylinodole (DAPI) (Molecular Probes Invitrogen, Eugene, OR, USA) to reveal cell nuclei. Images were obtained using a confocal fluorescence microscope (Zeiss LSM700, Munchen, Germany).

TUNEL Assay

Longitudinal cross-sections were cut 10-µm thick for in situ TdT-mediated dUTP nick end labeling assays (TUNEL) (Roche Diagnostics GmbH, Roche Applied Science, Mannheim, Germany); staining was performed with the fluorescein-tagged apoptosis detection system. Results were analyzed with a confocal microscope (Zeiss LSM700) at 488 nm wavelength.

Investigative Ophthalmology & Visual Science

Electroretinography

Mice underwent dark adaptation for 24 hours. Under dim red illumination, mice were anesthetized, and pupils were dilated with phenylephrine hydrochloride 10% (Efrin; Fischer Pharmaceutical Laboratories, Bnei Brak, Israel) and tropicamide 0.5% (Mydramide; Fischer Pharmaceutical Laboratories). Topical anesthesia was induced with drop of oxybuprocaine hydrochloride 0.4% (Localin; Fischer Pharmaceutical Laboratories). Eyes were bathed with 1.4% hydroxyethylcellulose (Celluspan; Fischer Pharmaceutical Laboratories) to keep corneas hydrated and to facilitate electrical conductivity. Active recording electrodes (LKC Technologies, Gaithersburg, MD, USA) were placed onto the corneas, and stainless-steel reference and ground electrodes were positioned subcutaneously on the ears and lower back.

ERG responses were recorded with the UTAS 3000 electrophysiology system (LKC Technologies, MD, USA), which uses a Ganzfeld light source with a maximum intensity of 5.76 cd-s/m^2. Several responses elicited by identical flashes at 2 to 30-second intervals were averaged. The amplitudes of the dark-adapted b-wave for experimental and control eyes were plotted as a function of log flash strength, and Vmax was derived as described in reference.[17] The ratios of maximal ERG a-wave to b-wave amplitudes for experimental versus control eyes were calculated at each time point.

Particle Induced X-Ray Emission (PIXE)

PIXE analysis was used to determine cobalt levels in biological fluids (blood, urine, and tears), as previously described.[18] In brief, standard cobalt solutions (1–200 mg/L) were prepared in 1% nitric acid for method validation, including sample homogeneity, dynamic range, and calibration curve determination. Multi-elemental analysis of dried matrix spots from small sample volumes (50 µL) with internal standard addition was performed.

PIXE measurements were analyzed with a 2.6 MeV proton beam from a 1.7 MV Pelletron Accelerator, using a FAST SDD detector with a 12 µm Mylar foil for filtration. Vanadium (20 µg/mL) served as an internal marker. Samples were irradiated to a total charge of 5 µC, and the GUPIX software (version 3.0.3) was used for spectrum analysis.

Electron Microscopy

The extracted optic nerves were dissected and placed in the fixation solution containing 2% glutaraldehyde and 2% paraformaldehyde in 0.1 M sodium cacodylate buffer for one hour at room temperature and then moved to 4°C for 16 hours. The samples were washed, post fixed with 1% osmium tetroxide containing 0.5% potassium dichromate and 0.5% potassium hexacyanoferrate for one hour, washed and en-bloc stained with 2% uranyl acetate for 60 minutes. After dehydration using ethanol, the tissue was infiltrated for three days with Epon812, oriented in silicon molds and polymerized at 60°C. Transverse ultra-thin 80 nm sections were cut using ultramicrotome UC7 (Leica, Wetzlar, Germany), transferred to copper grids, and viewed using a Talos L120C Transmission Electron Microscope (ThermoFisher, St. Louis, MO, USA) at an accelerating voltage of 120 kV.

Data analysis

GFAP Immunofluorescence Quantification. GFAP immunofluorescence intensity was quantified using ImageJ software, 1.54f (National Institutes of Health, Bethesda, MD, USA). Identical parameters of laser configuration and areas sampled for analysis were ensured. The areas of interest were marked with a rectangle drawn from the apical surface of the ganglion cell layer to the basal surface of the outer nuclear layer (ONL), from which mean fluorescence intensity for each retina was then collected.[19]

Quantification and Analysis of Retinal and Optic Nerve Iba1 Positive Cells. Z-stacks images of Iba1 positive cells of the retina and optic nerve sections were acquired using Zeiss LSM-700 (LSM700, Munchen, Germany) confocal microscopy using 20X objective. Imaging parameters and software set-up remained constant for all photomicrograph acquisition in the experiment. FIJI ImageJ software, 1.54f, was used for manual morphological analysis and the Sholl analysis plugin.[20,21]

Statistical Analysis

Statistical analyses were performed using GraphPad Prism (v.10.2.0; GraphPad Software, San Diego, CA, USA). One-way ANOVA with Tukey's multiple comparison tests was used for ERG, microglial morphometric analysis, and GFAP analysis. A significance level of $P < 0.05$ was applied to all statistical tests.

Results

Cobalt Levels in Blood, Urine, and Tears

PIXE analysis was used to ascertain cobalt levels in blood, urine, and tears. After a single IV injection of $CoCl_2$, cobalt levels decreased in blood over the first two hours (to less than 500 µg/L) while cobalt excretion in urine peaked after 90 min (370 g/L) (Supplementary Fig. S1). After daily IP injection, cobalt blood levels were very high (20–75 g/L), with significant variation among mice. However, in tears, cobalt injected by any route was below the PIXE detection level.

Cobalt-Induced Damage to the Retina and Optic Nerve

IV Injections—Macroscopic and Histologic Findings. High-dose IV injection of cobalt was immediately lethal in almost all cases. The mice that survived had macroscopically black optic nerves compared to non-injected eyes (Figs. 2A, 2F). Histological examination showed retinal distortion affecting all layers with severe inflammatory infiltrates, contrasting with the preserved retinal architecture observed in the control mice (Figs. 2B, 2C, 2G, 2H). The inflammatory reaction around the optic nerve intensified, with invading inflammatory cells noted within the nerve compared to the control (Figs. 2D, 2E, 2I, 2J).

Low-dose IV injections of cobalt were well tolerated. Histology sections examined 30 and 120 minutes after injection did not show noticeable changes in the retina or nerve compared to controls. All retinal layers were preserved. There was no inflammatory infiltration in the nerve.

Investigative Ophthalmology & Visual Science

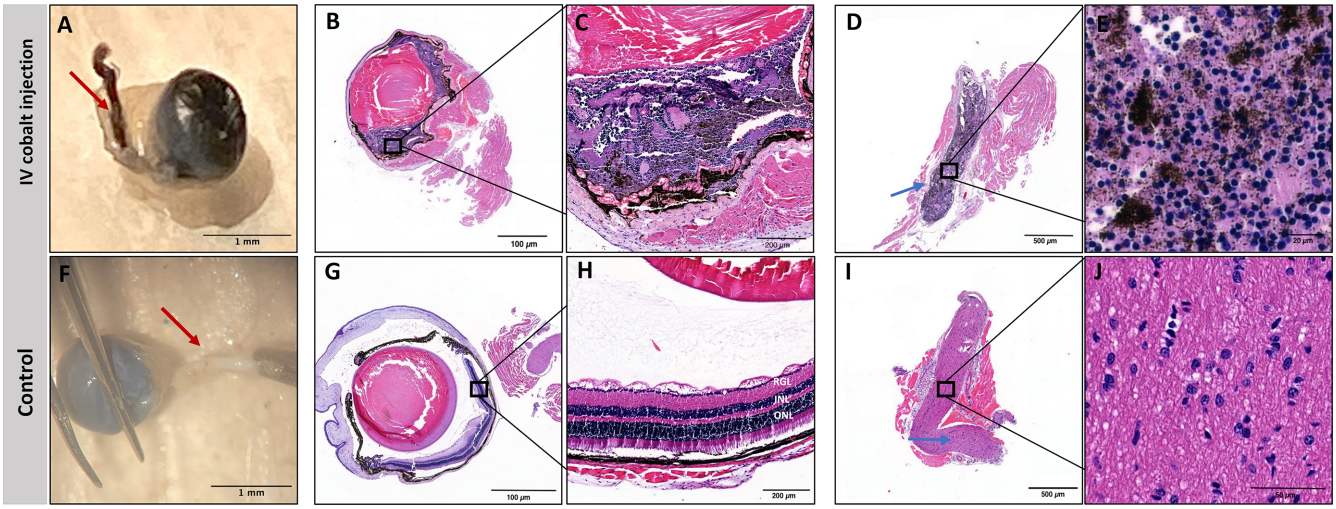

Figure 2. High-dose cobalt injection caused cellular infiltration into the retina and optic nerve. Macroscopic image showing a black optic nerve (*red arrow*) after three days of high dose IV cobalt administration **(A)**, compared to a normal optic nerve (*red arrow*) in a control mouse **(F).** H&E staining demonstrating cellular infiltration into the retina and the optic nerve of cobalt-injected mice at a low **(B**, **D)** and high **(C**, **E)** magnification, respectively (*blue arrow*, optic nerve), compared to normal retina and optic nerve in control mice at low **(G**, **I)** and high **(H**, **J)** magnification, respectively (*blue arrow*, optic nerve).

IP Injections—Macroscopic and Histologic Findings. Daily high-dose IP injections were lethal within three days. Mice that received a low IP dose survived.

Macroscopically, in mice that received a high daily dose IP for three days, the optic nerve appeared black. Histological sections prepared after three days showed retinal necrosis in addition to an inflammatory reaction surrounding the optic nerve, with complete inflammatory infiltration of the nerve in some cases (Supplementary Fig. S2). These cells were CD45 positive. CD45 is notably expressed on T- and B-lymphocytes, macrophages, and other immune cell types, making it a widely used marker in immunohistochemistry for identifying and quantifying inflammatory cells in tissues. However, it is absent on mature erythrocytes and platelets, which helps in distinguishing these immune cells from other non-nucleated blood components. CD45 immunostaining was used in this study to identify and localize inflammatory cells within the tissue, specifically to track immune cell infiltration in response to cobalt exposure. The presence of CD45-positive cells indicates the migration of immune cells, such as lymphocytes, macrophages, or other leukocytes, into the affected areas, which is a sign of inflammation. By targeting CD45, the staining specifically marks the inflammatory cells, allowing to assess the extent of inflammation and immune cell infiltration in the tissue (Supplementary Fig. S2). There was no inflammatory infiltration of the optic nerve in mice injected with a low IP dose for two, four, and eight weeks. Relative to controls, daily low-dose IP injection was associated with thinning of the ONL (48 ± 4.77 vs. 58 ± 4.925; $P < 0.05$) and INL (33 ± 4.81 vs. 43 ± 3.481, respectively; $P < 0.05$) after two months, in addition to a decrease in RGC count (33 ± 4.2 vs. 39 ± 3.726 in 300 µm; $P < 0.05$).

Immunohistochemistry. Iba-1 expression increased in the retina and the optic nerve after three days of daily high-dose injection. Iba-1 is a well-established marker for activated microglia and macrophages. Increased Iba-1 expression indicates an inflammatory response, specifically microglial activation. Iba-1 staining was used to identify and assess the microglia activation state in response to the high-dose cobalt injections. Signs of microglial/macrophage activation were evident, including increased soma size, increased circularity index and sholl intersections (Fig. 3). However, after four and eight weeks of daily low-dose cobalt, Iba-1–positive cells showed mild activation (Fig. 3).

GFAP is a key intermediate filament protein found in astrocytes and in Müller cells. It serves as a crucial marker for astrocyte activation and reactive gliosis, a process where glial cells proliferate and undergo hypertrophy in response to injury or stress. Increased GFAP indicates reactive gliosis which is a hallmark of neuroinflammation. GFAP immunostaining in our study showed increased intensity in the retina and optic nerve after three days of high dose IP daily cobalt injection. Increased GFAP immunostaining was also noticed although to a lesser extent after 8 weeks of daily low dose IP cobalt injection (Figs. 4A, 4B).

Myelin basic protein immunostaining demonstrated demyelination in the optic nerves after 56 days of daily low dose cobalt treatment (Fig. 5B). NeuN immunostaining of the retinal sections which specifically labels retinal ganglion cells, confirmed RGC loss in the cobalt daily low dose–treated group as shown in Figure 4D.

TUNEL Assay. High-dose IP injection caused necrosis of the retina, with negative TUNEL staining. After daily low-dose IP injections for four weeks, apoptotic cells were detected in the peripheral regions of the retina. At eight weeks, apoptotic cells were found in all retinal layers (RGC layer, INL, ONL) (Fig. 4C). There was no apoptosis of oligodendrocyte cells in the optic nerve.

Electron Microscopy. Transmission electron microscopy demonstrated optic nerve damage after eight weeks of daily low dose IP cobalt injections. Signs of optic nerve damage such as axonal enlargement and demyelination, swollen axonal and astrocytic mitochondria, condensed electron opaque axoplasm, and axons filled with cellular debris were all highly evident in comparison with control mice that showed intact and uniformly myelinated axons (Figs. 5A1–A6).

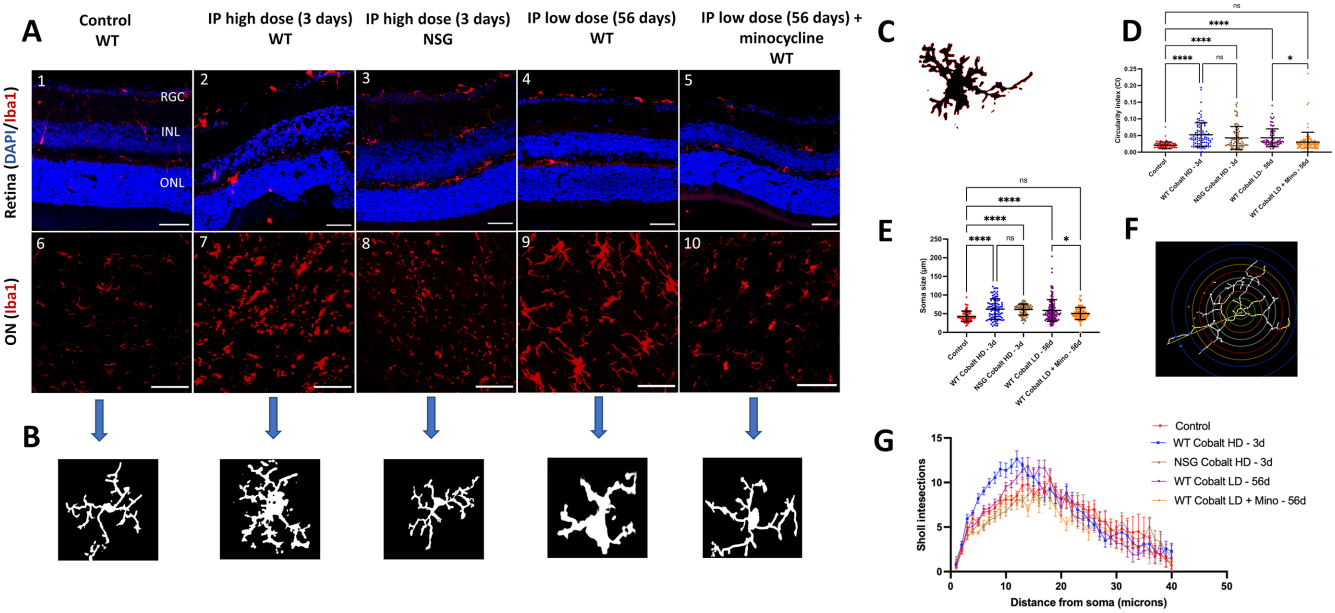

Figure 3. Microglial morphometric analysis. **(A, B)** Microglial morphometric analysis was used to identify the activation state of microglia caused by cobalt toxicity. **(C)** A graphical representation depicting the calculation bases for the circularity index (CI). **(D, E)** Plot showing CI value and soma size (µm) in the different groups of the experiment, with each *dot* representing a single cell. **(F, G)** A distinct differentiation among the group becomes evident by examining how the distribution of Sholl intersection varies with distance from the soma. Analysis was performed by one-way ANOVA with Tukey's multiple comparison tests. Fifteen to twenty cells per region of 5 mice for each group ($n = 5$). Statistical significance indicated with asterisks: *$P < 0.05$, ****$P < 0.0001$. HD, high dose; LD, low dose; Mino, minocycline.

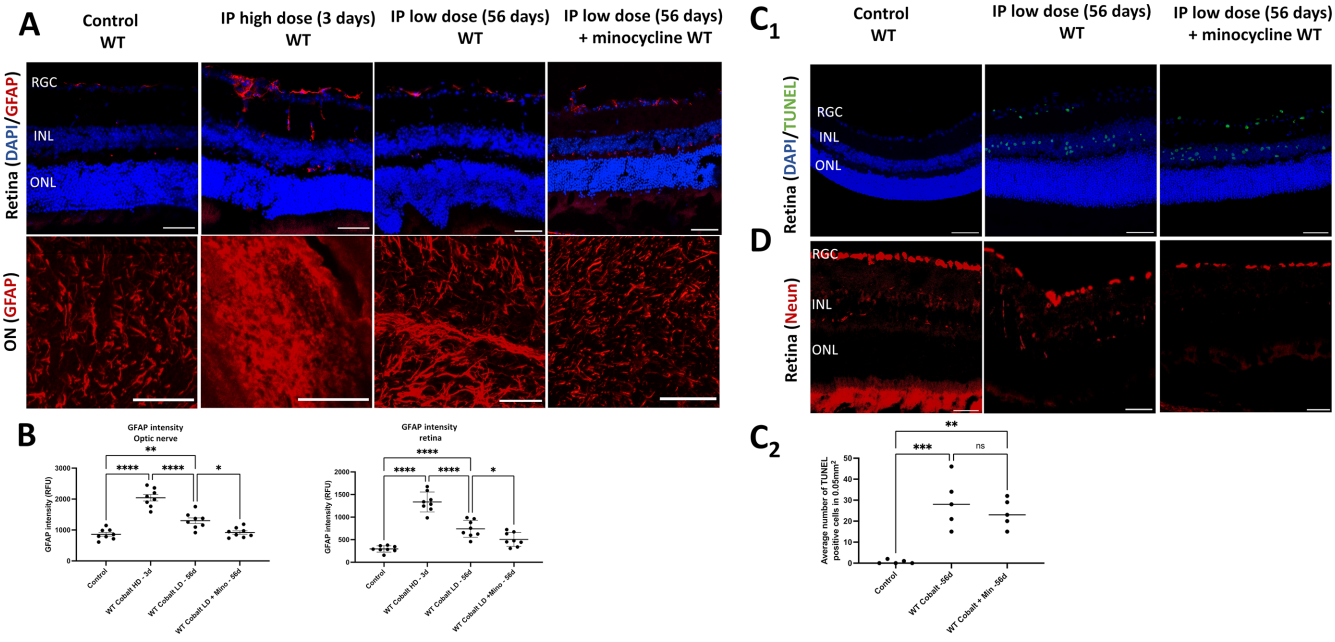

Figure 4. Cobalt toxicity caused increased gliosis and apoptotic reaction. **(A, B)** IP injection of cobalt chloride induced gliotic reaction in the retina and the optic nerve (DAPI, *blue*; GFAP, *red* immunostaining). **(A)** Immunostaining for GFAP showed evident gliosis of the optic nerve and retina after three days of daily IP high-dose cobalt injection compared to control mice, and to a lesser extent IP low dose daily after 56 days. **(B)** Quantification of GFAP mean fluorescence intensity showed higher amount of immunoreactivity for the cobalt-injected group in both the retina and optic nerve whereas the minocycline injection had a negative effect on GFAP activation in the retina and the optic nerve ($n = 5$, per group) with eight retinas in total for each group. **(C)** TUNEL staining to detect apoptosis. Minimal staining in control mice, while positive apoptotic staining detected after 8 weeks of daily low dose IP cobalt chloride injection, mainly in the ganglion cell layer and INL layers. Positive staining was also noted in the minocycline-treated group ($n = 5$, per group). **(D)** NeuN staining confirmed RGC loss in the cobalt treated group. *Scale bar*: 50 µm. Statistical analysis was performed by one-way ANOVA with Tukey's multiple comparison tests. *$P < 0.05$, **$P < 0.01$, ***$P < 0.001$, ****$P < 0.0001$.

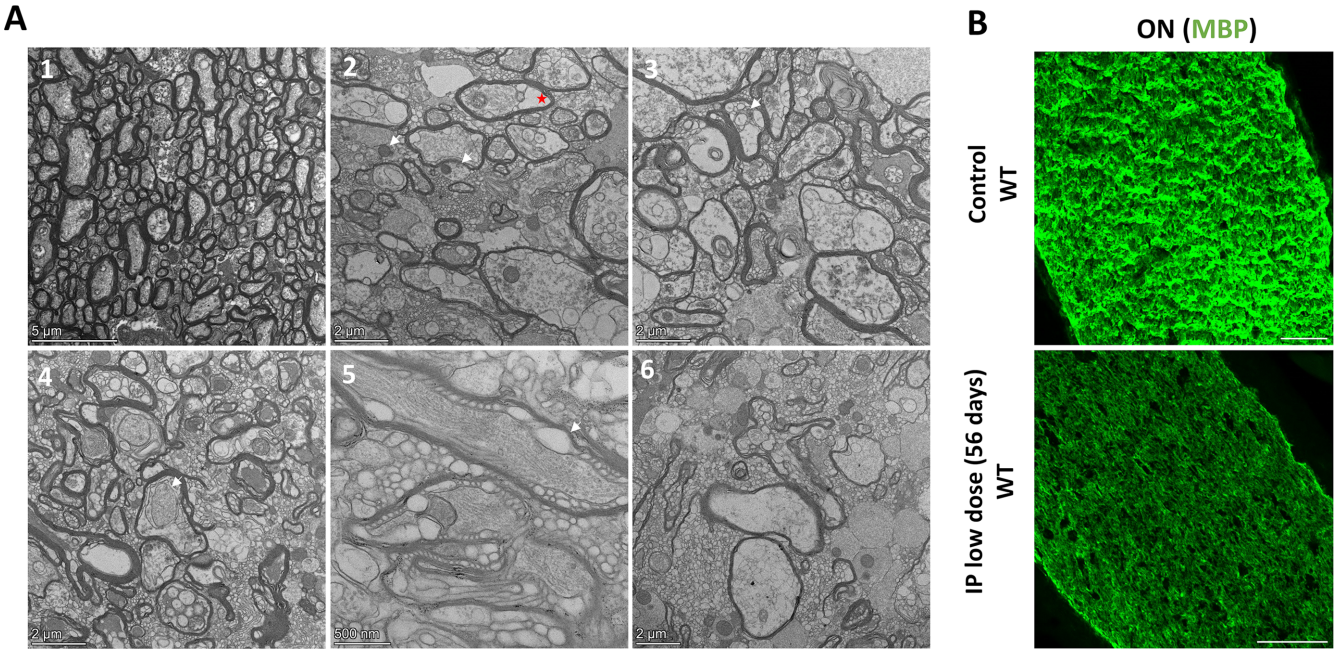

Figure 5. Identification of degenerating optic nerve axons using transmission electron microscopy and myelin staining. Transmission electron microscopy of optic nerve in control mice (**A1**) and after eight weeks of daily low-dose IP cobalt injections (**A2–A6**). (**A1**) Uniformly myelinated axons in control mice. (**A2**) Degenerating axons can be identified by condensed electron opaque axoplasm (*white arrow*) and edema (red asterisk). (**A3**, **A4**) Axons can be filled with cellular debris (*white arrow*) **(A3)** and may have swelling and degeneration of axonal mitochondria (*white arrow*) (**A4**). (**A5**, **A6**) Chronic cobalt toxicity caused enlarged astrocytic mitochondria (*white arrow*) (**A5**) and enlarged and demyelinated axons with empty axonal myelin sheath (**A6**). (**B**) Myelin basic protein (MBP) staining showing demyelination after 56 days of daily IP low dose cobalt injection; *Scale bar*: 50 µm.

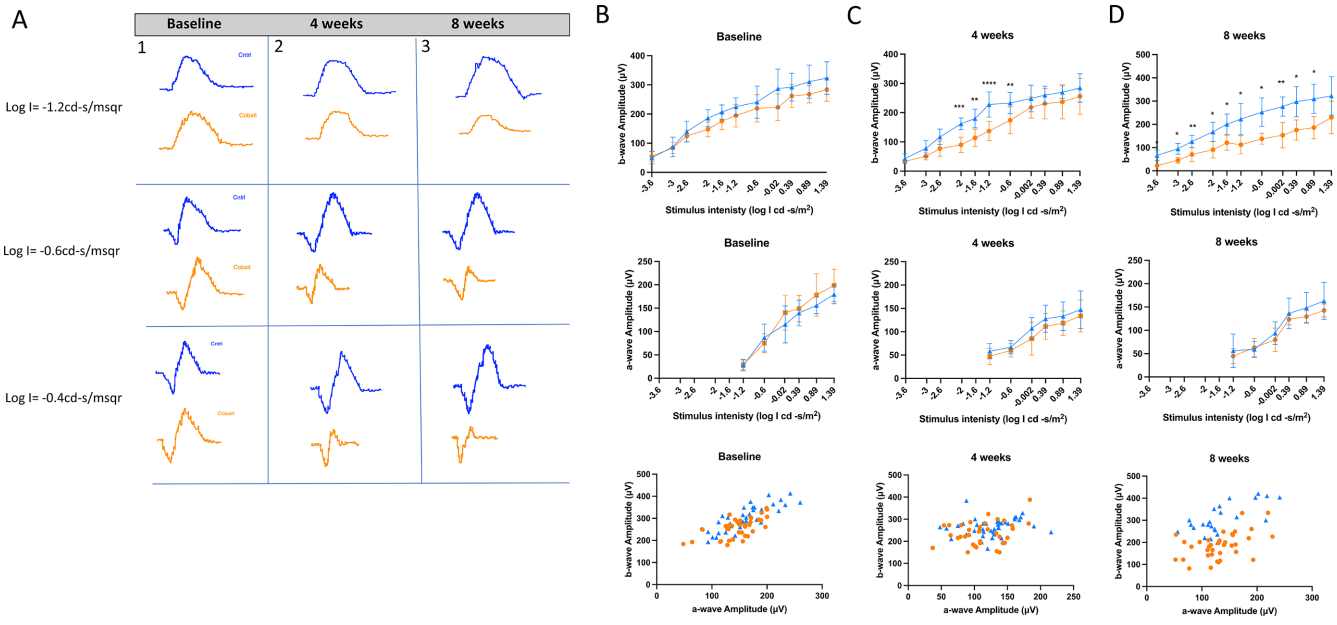

Figure 6. Schematic of in vivo ERG analysis. (**A1–A3**) Schematic ERG representation of the average values at different light intensities at baseline (**A1**), after four weeks (**A2**), and eight weeks (**A3**) of cobalt injection for both control and injected groups. (**B–D**) Response stimulus strength relation ERG for mice at baseline, after four weeks, and after eight weeks of cobalt injection showed a gradual decrease of the b-wave amplitude and the relation between the b-wave to a-wave in the injected group (*orange circle*) compared to the non-injected group (*blue triangle*). The analysis was performed by one-way ANOVA comparison test. ($n = 10$, per group), $^{*}P < 0.05$;$^{**}P < 0.01$; $^{***}P < 0.001$; $^{****}P < 0.0001$.

IP Injections—ERG. Functional ERG studies were performed at baseline, after four weeks, and after eight weeks in mice injected IP with a low dose of cobalt and sham control mice (Fig. 6). At baseline, the ERG responses were similar between the experimental and control eyes in both groups. After four to eight weeks of repeated daily injections, mice that received cobalt showed a significant reduction in mean b-wave values compared to controls, with

a greater reduction in b-wave amplitude after eight weeks (Fig. 6).

NSG Mice

NSG mice were injected with low dose IV cobalt ($n = 8$) to determine the pharmacokinetics of cobalt in immunodeficient mice. PIXE analysis revealed that, over time, the changes in blood and urine cobalt concentrations were comparable to those observed in WT mice.

NSG mice were injected with high dose cobalt IP daily for three days ($n = 9$) to identify acute cobalt-related tissue response such as inflammation. Morphological and signal quantification and analysis of Iba1 showed reduced microglial activation in the retina and optic nerves in the NSG mice compared to WT (Figs. 3).

Minocycline Did Not Ameliorate Optic Nerve and Retinal Gliosis Due to Cobalt Toxicity

The potential therapeutic effect of minocycline, a broad-spectrum tetracycline antibiotic with well-documented anti-inflammatory properties, was evaluated in the cobalt toxicity model. Minocycline is recognized as a potent inhibitor of microglial activation, which is a key contributor to neuroinflammation based on the immunohistochemical findings of activated microglial cells in the retina and optic nerve in our model. Minocycline was administered to assess its ability to attenuate this microglial response, with the aim of reducing the associated neuroinflammation and potential neuronal damage, thus offering a protective effect. Cobalt and minocycline have been injected simultaneously IP for 56 days. Minocycline treatment resulted in a reduction in the activation of Iba1-positive cells (Fig. 3) and had significant effect on gliosis (Figs. 4A, 4B). In contrast, TUNEL-positive cell counts in the retina in the minocycline treated group was similar to the cobalt only group (Fig. 4C).

Discussion

Using advanced multimodal technologies, the present study provides direct evidence of the toxic anatomical and functional effects of cobalt on the visual system in a mouse model. Several studies and case reports have shown that both the retina and the optic nerve are affected by cobalt toxicity, either transiently or permanently.[1,5,13,22] However, attempts to elucidate the underlying mechanisms often led to inconclusive results,[22,23] mostly because of technical difficulties in detecting trace levels of cobalt in animal tissues and body fluids and the lack of an animal model of chronic cobalt toxicity.

Between IV and intraperitoneal IP cobalt injections at different concentrations, the IV method showed rapid urinary elimination of cobalt, whereas PIXE measurements revealed elevated cobalt levels in the blood following chronic IP injection. Additionally, PIXE technology was used to measure cobalt levels in tears. Unlike other analytical methods, PIXE allows for simultaneous multi-elemental analysis with high sensitivity and spatial resolution, making it particularly suitable for investigating the distribution and accumulation of cobalt in various biological samples and tissues. The inflammatory and toxic effect of cobalt on the ocular tissues was investigated following systemic induction of cobalt toxicity for a short period with high dose leading to sudden increase of cobalt levels, mimicking a situation of sudden hip implant rupture, and for a longer period with a low dose causing gradual increase of cobalt levels as slow release from the hip implant or chronic occupational exposure. Different imaging and functional modalities including ERG, in addition to histologic, immunohistochemical, and molecular studies were used to investigate the effect of cobalt toxicity on the visual system.

In the IV model, cobalt was nearly eliminated from the mouse body shortly after a single IV injection. In contrast, in the IP model, cobalt concentrations in the blood remained elevated for a longer period, making the IP route more suitable for a sustained systemic cobalt toxicity model similar to clinical scenarios. This difference might be attributed to the slow diffusion of cobalt through the peritoneum. The IP administration of cobalt resulted in significant damage to ocular tissues, specifically affecting the retina and optic nerve. Ocular inflammation was more prominent in high- versus low-dose IP cobalt administration. In the retina, cobalt appeared to trigger apoptosis and at higher doses necrosis, leading to photoreceptor degeneration over time. Low doses had a progressive functional effect on vision, and higher doses led to rapid extensive ocular damage perhaps involving an aggressive inflammatory reaction induced directly by cobalt or its hypoxic effects (inflammation due to ischemia).

Apostoli et al.[22] found RGCs depletion, diffuse areas of optic nerve damage, and axonal swelling following daily IV infusion of cobalt in rabbits. The severity of the damage was associated with the dose and duration of exposure. In the present study, systemic administration of high-dose cobalt, either IV or IP, led to a massive inflammatory reaction in both the retina and optic nerve that was mainly microglial/macrophage-driven, with signs of gliosis.

After IP cobalt administration, ERG configuration revealed a decreased correlation between the a-wave (reflecting photoreceptor layer integrity) and the b-wave (originating from retinal cells postsynaptic to photoreceptors). Procedures that block synaptic transmission, such as cobalt ion super-perfusion or high-magnesium/low-calcium solutions, can eliminate the b-wave and isolate the PIII component.[17] Normal a- and b-wave relationships indicate proper signal transmission in the distal retina, while an abnormal b-to-a wave ratio signals outer plexiform layer dysfunction. Our study observed an abnormal b-to-a wave ratio, consistent with earlier findings in frogs showing complete elimination of rod-photoreceptor contributions to the ERG-b wave after cobalt exposure.[24] In our mouse model, the reduced b-wave amplitude at eight weeks, alongside a normal a-wave amplitude, suggests potential postsynaptic dysfunction or a reduction in photoreceptors.

As anticipated, the photoreceptors were highly sensitive to hypoxia because of the high oxygen consumption of their inner segments.[25] This necessitates a constant oxygen supply via retinal circulation to preserve retinal function. Cobalt, due to its hypoxic effect, is involved in HIF2 elevation.[26] As described by Maslim et al.,[25,27] photoreceptor death and survival are strongly influenced by tissue oxygen levels, especially during a critical period in their development.

At eight weeks after daily IP cobalt administration, TEM analysis revealed nerve damage and degeneration characterized by myelin loss, edema, and enlarged mitochondria. Histologically, infarcts were observed alongside vacuolization and disruption of the optic nerve architecture. Retinal thinning was also noted. Apoptosis assays yielded a positive

Investigative Ophthalmology & Visual Science

signal in the retina after almost four weeks of daily low-dose cobalt administration. The relative number of TUNEL positive ganglion cells increased at week 8. This delayed loss of RGCs might be explained by the higher sensitivity of photoreceptors to hypoxia.[25,27]

Metal-on-metal hip arthroplasty has been associated with the development of inflammatory reactions[28–30] and acute lymphocyte-dominated vasculitis-associated lesions.[31] Lawrence et al.[32] demonstrated a connection between cobalt and activation of the Toll-like 4 immune receptors, leading to an inflammatory response and increased release of pro-inflammatory cytokines.[33] It is noteworthy that $CoCl_2$ can directly induce an inflammatory response, characterized by enhanced expression of IL-6 and IL-8 in endotheliocytes and astrocytes[34] in addition to overexpression of IL-1β and TNFα in fibroblasts.[35] In our study cobalt IV/IP injection led to an inflammatory reaction in the retina and optic nerve; even in the immunodeficient NSG mice, cobalt activated microglia in the optic nerve and, to a lesser extent, in the retina, which can result in tissue damage.

Reactive gliosis, which is present in virtually all forms of retinal injury or disease, was highly evident after high-dose IP or chronic administration.[36] Muller glia, the major glial cells to maintain retinal homeostasis, are activated and rearranged immediately in response to photoreceptor stress in a phenomenon collectively known as retinal remodelling.[37] Although Muller cell activation in response to $CoCl_2$ represents a defense mechanism, capable of clearing cobalt from the retina, it might also disrupt retinal homeostasis and play a secondary role in cobalt-mediated retinal toxicity.

On the macroscopic level, following systemic administration of high-dose cobalt, the optic nerve appeared black. Histology showed an infiltrating inflammatory reaction mainly with mononuclear cells, confirmed by immunoreactivity to Iba-1 and CD45 staining. Iba-1 is a specific calcium-binding protein with actin-bundling activity that participates in membrane ruffling and phagocytosis in activated microglia. The Iba-1-positive microglial cells showed typical signs of activation such as increased cell body size and decrease in branch length. Microglial activation was also noted after chronic low-dose IP administration, although to a lesser extent. This suggests that microglial activation might play a partial role in the damage induced by cobalt toxicity.

Assuming that the cobalt induced pathology could be partially influenced by the activated microglial cells, the potential therapeutic impact of minocycline, a potent inhibitor of microglial activation, was explored.[38] Minocycline treatment reduced the activation of Iba1 positive cells and optic nerve gliosis, but not the apoptosis in cobalt-injected mice.

In summary, this study provides valuable insights into the pathophysiology of cobalt-induced ocular toxicity and presents substantial evidence for the in vivo pathological effects of cobalt on the retina and optic nerve. It is important to highlight that the detection of metallosis currently faces challenges due to the lack of highly sensitive techniques. Using PIXE, we demonstrated both high specificity and sensitivity for metal detection. Moving forward, the integration of such advanced methods into medical practice should be strongly considered.

Acknowledgments

The authors thank Irit Mann and Ido Perlman for their critical revision and assistance with the ERG data. In addition, we express our sincere appreciation to the dedicated and knowledgeable staff at the BCF (Biochemical Core Facility) of the Technion institute, mainly Galit Saar and Maya Holdengreber, for their invaluable support and expertise throughout the course of this research project.

This work was presented in part at the Israeli Society for Vision and Eye Research (ISVER) March 2022, March 2023, Tel Aviv, Israel; North American Neuro-Ophthalmology Society (NANOS) March 2023, Orlando, FL, USA; The Association for Research in Vision and Ophthalmology (ARVO) April 2023, New Orleans, LA, USA; European Society of Ophthalmology (ESO) June 2023, Prague, Czech Republic; and the 2nd Global Summit on Nanotechnology and Materials Science – GSNMS-September 2023, Rome, Italy. European Neuro-opthalmology Society (ENOS), Roterdam, Holland June 2024.

Supported by the Israel Scientific Foundation (ISF) grant No. 2509/21 (N.G-C.); the Zanvyl and Isabelle Krieger Fund, Baltimore, MD (N.G-C.). The funding organization had no role in the design or conduct of this research.

Author Contributions: Conceptualization, B.O, A.Z., O.G., and N.G.-C.; methodology and investigation, B.O, S.R, A.Z., O.G., M.K, H.K.-S., J.B., D.F, and N.G.-C; writing original draft preparation and review and editing, B.O, A.Z., S.R, O.G., and N.G.-C; supervision, A.Z., S.R, O.G. and N.G.-C.; funding acquisition, N.G.-C. All authors have read and agreed to the published version of the manuscript.

Ethics Approval: Mice were maintained and handled in accordance with the Association for Research in Vision and Ophthalmology (ARVO) Statement for the Use of Animals in Ophthalmic and Vision Research and the National Institutes of Health guidelines. All animal protocols used in the study were approved by the local Animal Research Committee at Rabin Medical Center, Israel (RMC_02062021). The study is reported in accordance with ARRIVE guidelines.

Disclosure: **B. Obied**, None; **S. Richard**, None; **A. Zahavi**, None; **H. Kreizman-Shefer**, None; **J. Bajar**, None; **D. Fixler**, None; **M. Krmpotić**, None; **O. Girshevitz**, None; **N. Goldenberg-Cohen**, None

References

1. Tower SS. Arthroprosthetic cobaltism: neurological and cardiac manifestations in two patients with metal-on-metal arthroplasty: a case report. *J Bone Joint Surg Am.* 2010;92:2847–2851.
2. Garcia MD, Hur M, Chen JJ, Bhatti MT. Cobalt toxic optic neuropathy and retinopathy: Case report and review of the literature. *Am J Ophthalmol Case Rep.* 2020;17:100606
3. Leyssens L, Vinck B, van der Straeten C, Wuyts F, Maes L. Cobalt toxicity in humans—a review of the potential sources and systemic health effects. *Toxicology.* 2017;387:43–56.
4. Alexander CS (1972) Cobalt-beer cardiomyopathy. A clinical and pathologic study of twenty-eight cases. *Am J Med.* 1972;53:395–417.
5. Grillo LM, Nguyen HV, Tsang SH, Hood D C, Odel JG. Cobalt-chromium metallosis with normal electroretinogram. *J Neuroophthalmol.* 2016;36:383–388.
6. Rizzetti MC, Liberini P, Zarattini G, et al. Loss of sight and sound. Could it be the hip? *Lancet.* 2009;373(9668):1052.
7. Apel W, Stark D, Stark A, O'Hagan S, Ling J. Cobalt-chromium toxic retinopathy case study. *Doc Ophthalmol.* 2013;126:69–78.
8. Dahms K, Sharkova Y, Heitland P, Pankuweit S, Schaefer JR. Cobalt intoxication diagnosed with the help of Dr House. *Lancet.* 2014;383(9916):574.

9. Harris A, Johnson J, Mansuripur PK, Limbird R. Cobalt toxicity after revision to a metal-on-polyethylene total hip arthroplasty for fracture of ceramic acetabular component. *Arthroplast Today.* 2015;1(4):89–91.
10. Ho VM, Arac A, Shieh PB. Hearing and vision loss in an older man. *JAMA Neurol.* 2018;75:1439–1440.
11. Ng SK, Ebneter A, Gilhotra JS. Hip-implant related chorioretinal cobalt toxicity. *Indian J Ophthalmol.* 2013;61:35–37.
12. Peters RM, Willemse P, Rijk PC, Hoogendoorn M, Zijlstra WP. Fatal cobalt toxicity after a non-metal-on-metal total hip arthroplasty. *Case Rep Orthop.* 2017;2017:9123684
13. Steens W, von Foerster G, Katzer A. Severe cobalt poisoning with loss of sight after ceramic-metal pairing in a hip–a case report. *Acta Orthop.* 2006;77:830–832.
14. Weber KP, Schweier C, Kana V, Guggi T, Byber K, Landau K. Wear and tear vision. *J Neuroophthalmol.* 2015;35:82–85.
15. Zheng F, Li Y, Zhang F, et al. Cobalt induces neurodegenerative damages through Pin1 inactivation in mice and human neuroglioma cells. *J Hazard Mater.* 2021;419:126378
16. Morita Y, Itokazu T, Nakanishi T, Hiraga SI, Yamashita T. A novel aquaporin-4-associated optic neuritis rat model with severe pathological and functional manifestations. *J Neuroinflammation.* 2022;19:263.
17. Perlman I. The Electroretinogram: ERG. In: Kolb H, Fernandez E, Nelson R, editors. *Webvision: The Organization of the Retina and Visual System*. Salt Lake City (UT): University of Utah Health Sciences Center, 2001.
18. Girshevitz O, Cohen-Sinai N, Zahavi A, Vardizer Y, Fixler D, Goldenberg-Cohen N. Trace elements in tears: Comparison of rural and urban populations using particle induced X-ray emission. *J. Pers. Med.* 2022;12:1633.
19. Jiao H, Provis JM, Natoli R, Rutar M. Ablation of C3 modulates macrophage reactivity in the outer retina during photooxidative damage. *Mol Vis.* 2020;26:679–690.
20. Young K, Morrison H. Quantifying microglia morphology from photomicrographs of immunohistochemistry prepared tissue using ImageJ. *J Vis Exp.* 2018;(136):57648.
21. Heindl S, Gesierich B, Benakis C, Llovera G, Duering M, Liesz A. Automated morphological analysis of microglia after stroke. *Front Cell Neurosci.* 2018;12:106.
22. Apostoli P, Catalani S, Zaghini A, et al. High doses of cobalt induce optic and auditory neuropathy. *Exp Toxicol Pathol.* 2013;65:719–727.
23. Hara A, Niwa M, Aoki H, et al. A new model of retinal photoreceptor cell degeneration induced by a chemical hypoxia-mimicking agent, cobalt chloride. *Brain Res.* 2006;1109:192–200.
24. Evans JA, Hood DC, Holtzman E. Differential effects of cobalt ions on rod and cone synaptic activity in the isolated frog retina. *Vis Res.* 1978;18:145–151.
25. Maslim J, Valter K, Egensperger R, Holländer H, Stone J. Tissue oxygen during a critical developmental period controls the death and survival of photoreceptors. *Invest Ophthalmol Vis. Sci.* 1997;38:1667–1677.
26. Muñoz-Sánchez J, Chánez-Cárdenas ME. The use of cobalt chloride as a chemical hypoxia model. *J Appl Toxicol.* 2019;39:556–570.
27. Valter K, Maslim J, Bowers F, Stone J. Photoreceptor dystrophy in the RCS rat: roles of oxygen, debris, and bFGF. *Invest Ophthalmol Vis Sci.* 1998;39:2427–2442.
28. Bosker BH, Ettema HB, Boomsma MF, Kollen BJ, Maas M, Verheyen CC. High incidence of pseudotumour formation after large-diameter metal-on-metal total hip replacement: a prospective cohort study. *J Bone Joint Surg Br.* 2012;94:755–761.
29. Daniel J, Holland J, Quigley L, Sprague S, Bhandari M. Pseudotumors associated with total hip arthroplasty. *J Bone Joint Surg Am.* 2012;94:86–93.
30. van der Weegen W, Brakel K, Horn RJ, et al. Asymptomatic pseudotumours after metal-on-metal hip resurfacing show little change within one year. *Bone Joint J.* 2013;95-B:1626–1631.
31. Willert HG, Buchhorn GH, Fayyazi A, et al. Metal-on-metal bearings and hypersensitivity in patients with artificial hip joints. A clinical and histomorphological study. *J Bone Joint Surg Am.* 2005;87:28–36.
32. Lawrence H, Deehan D, Holland J, Kirby J, Tyson-Capper A. The immunobiology of cobalt: demonstration of a potential aetiology for inflammatory pseudotumours after metal-on-metal replacement of the hip. *Bone Joint J.* 2014;96-B:1172–1177.
33. Chow JC, Young DW, Golenbock DT, Christ WJ, Gusovsky F. Toll-like receptor-4 mediates lipopolysaccharide-induced signal transduction. *J Biol Chem.* 1999;274:10689–10692.
34. Mustoe TA, O'Shaughnessy K, Kloeters O. Chronic wound pathogenesis and current treatment strategies: a unifying hypothesis. *Plast Reconstr Surg.* 2006;117(7 Suppl):35S–41S.
35. Schmalz G, Schweikl H, Hiller KA. Release of prostaglandin E2, IL-6 and IL-8 from human oral epithelial culture models after exposure to compounds of dental materials. *Eur J Oral Sci.* 2000;108:442–448.
36. Nakazawa T, Takeda M, Lewis GP, et al. Attenuated glial reactions and photoreceptor degeneration after retinal detachment in mice deficient in glial fibrillary acidic protein and vimentin. *Invest Ophthalmol Vis Sci.* 2007;48:2760–2768.
37. Bringmann A, Pannicke T, Grosche J, et al. Müller cells in the healthy and diseased retina. *Prog Retin Eye Res.* 2006;25:397–424.
38. Kobayashi K, Imagama S, Ohgomori T, et al. Minocycline selectively inhibits M1 polarization of microglia. *Cell Death Dis.* 2013;4(3):e525.

Investigative Ophthalmology & Visual Science